Clim. Past, 19, 1295–1304, 2023
https://doi.org/10.5194/cp-19-1295-2023

Climate of the Past
Open Access
EGU

A comparison of pre-millennium eruption (946 CE) and modern temperatures from tree rings in Changbai Mountain, Northeast Asia

Haibo Du[1], Michael C. Stambaugh[2], Jesús Julio Camarero[3], Mai-He Li[1,4], Dapao Yu[5], Shengwei Zong[1], Hong S. He[2], and Zhengfang Wu[1]

[1]Key Laboratory of Geographical Processes and Ecological Security in Changbai Mountains, Ministry of Education, School of Geographical Sciences, Northeast Normal University, Changchun 130024, China
[2]School of Natural Resources, University of Missouri, Columbia, Missouri, USA
[3]Instituto Pirenaico de Ecología, IPE-CSIC, 50059 Zaragoza, Spain
[4]Swiss Federal Institute for Forest, Snow and Landscape Research WSL, 8903, Birmensdorf, Switzerland
[5]CAS Key Laboratory of Forest Ecology and Management, Institute of Applied Ecology, Chinese Academy of Sciences, Shenyang 110016, China

Correspondence: Zhengfang Wu (wuzf@nenu.edu.cn) and Hong S. He (heh@missouri.edu)

Received: 14 June 2022 – Discussion started: 1 November 2022
Accepted: 1 June 2023 – Published: 4 July 2023

Abstract. High-resolution temperature reconstructions in the previous millennium are limited in Northeast Asia, but they are important for assessing regional climate dynamics. Here, we present, for the first time, a 202-year reliable reconstruction of April temperature changes before the millennium volcanic eruption in 946 CE using tree rings of carbonized logs buried in the tephra in Changbai Mountain, Northeast Asia. The reconstructed temperature changes were consistent with previous reconstructions in China and the Northern Hemisphere. The influences of large-scale oscillations (e.g. El Niño–Southern Oscillation, ENSO) on temperature variability were not significantly different between the periods of 745–946 CE preceding the eruption and 1883–2012. However, compared to the palaeotemperature of the previous millennium, the temperature changes were more complex with stronger temperature fluctuations, more frequent temperature abruption, and a weaker periodicity of temperature variance during the last 130 years. These recent changes correspond to long-term anthropogenic influences on regional climate.

1 Introduction

The observed global mean surface temperature for the decade 2011–2020 was ∼1.09 °C higher than the average over the 1850–1900 period, reflecting the warming trend since the industrial period (IPCC, 2021). Century-wide predictions have been made based on relatively short-term observations, which bear great uncertainties especially at local and regional spatial scales. Different from the short instrumental records, reconstructing long-term climate variability using proxies resolved annually such as tree rings is important for analysing the long-term variations in climate and discriminating among natural and anthropogenic factors that drive climate change (Wang et al., 2018). Long-term dendroclimatic reconstructions of temperature are essential to validate global climate models and provide important inputs to understand vegetation succession and vegetation–climate relationships in the region (Schneider et al., 2015).

Tree rings are excellent proxies for high-resolution climate reconstruction (Fritts, 1976). Several millennial-scale annual climate reconstructions have been developed by multiproxy data for the globe (PAGES 2k Consortium et al., 2013; Mann et al., 2008; Mann and Jones, 2003), the Northern Hemisphere (Guillet et al., 2017; Moberg et al., 2005; Mann et al., 1999), or the Northern Hemisphere extratropical regions

(Schneider et al., 2015; Ljungqvist, 2010). Some millennial temperature reconstructions with very coarse temporal resolution using other proxies were also completed in Northeast Asia, e.g. using varved sediment in Lake Sihailongwan (42°17′53″ N, 126°36′59″ E) (Chu et al., 2012). However, the millennial-scale and high-resolution climate reconstructions rarely include tree-ring proxies from Northeast Asia due to limited available tree records prior to the last millennium.

The Changbai Mountain is the highest mountain in Northeast Asia and encompasses all life zones found along altitudinal gradients from temperate forests to the alpine tundra (Zhou et al., 2005). Tree radial growth is sensitive to climate change in Changbai Mountain which has allowed the building of several dendroclimatic reconstructions for the past centuries (Du et al., 2018; Lyu et al., 2016; Zhu et al., 2009; Shao and Wu, 1997). The highest peak of Changbai Mountain with origins from an intraplate stratovolcano (Tianchi volcano) is located on the border between China and North Korea (Sun et al., 2014). A Plinian eruption occurred around 1000 CE (well-known as the "Millennium Eruption") with a volcanic explosivity index of 7 based on an estimated eruptive column of ∼ 25–35 km and a total tephra volume of ∼ 100 km^3 (Wei et al., 2003; Horn and Schmincke, 2000). The eruption destroyed most plants within a ∼ 50 km radial area, but many trees buried by volcanic ash became carbonized logs (Cui et al., 1997). These carbonized logs provide a unique material to reconstruct climate of Changbai Mountain prior to the millennium eruption using tree-ring records as climate proxies.

Numerous studies have attempted dating of the Millennium Eruption (Chen et al., 2016; Xu et al., 2013; Yin et al., 2012). Recently, this eruption has been dated to the end of 946 CE using a conspicuous dating marker of the ephemeral burst of cosmogenic radiation in 775 CE (Oppenheimer et al., 2017; Büntgen et al., 2014) and historical documents (Yun, 2013). With this date, carbonized trees provide the opportunity to reconstruct climate before 946 CE in Changbai Mountain, a region where the greatest increase in air temperature over China was recorded during the last century (Ding et al., 2007).

Here, we analyse tree rings from the carbonized logs and modern trees on Changbai Mountain to reconstruct and compare temperatures between the 3 centuries pre-Millennium Eruption and the last 2 centuries (1883–2012). These temperature reconstructions can reveal the long-term regional climate dynamics in Northeast China or even Northeast Asia and allow characterizing recent features related to anthropogenic climate warming.

2 Material and methods

The Changbai Mountain ranges from 713 to 2691 m a.s.l., and it belongs to the temperate continental and mountain climate, with an annual mean temperature ranging from −7.3 to 4.9 °C and annual precipitation from 800 to 1800 mm (Du et al., 2018). The period of cambial growth of trees is approximately May to September at low altitudes (e.g. 1000 m a.s.l.) and shortens between June and August at high altitudes (e.g. treeline located at ∼ 2060 m a.s.l.) (Du et al., 2021).

We sampled 55 carbonized trees from two nearby sites on the western slope of Changbai Mountain in 2012 and 2013 (site A – 42°9′ N, 127°52′ E, 1025 m a.s.l., with 33 samples; and site B – 42°5.7′ N, 127°42.4′ E, 892 m a.s.l., with 22 samples) (Fig. 1a, b, c). Most of these trees had bark indicating that the last year of tree growth was present (Fig. 1d). Radiocarbon dating of the wood of the outermost rings of two trees (from sites A and B, respectively; Fig. 1a) was conducted in the accelerator mass spectrometry (AMS) laboratory at Peking University (Table 1) and indicated that these trees died during the Millennium Eruption in 946 CE. Other carbonized trees found and reported in previous studies were also dead in 946 CE (e.g. Oppenheimer et al., 2017; Xu et al., 2013; Yin et al., 2012). Many of these carbonized tree samples were not totally carbonized (Fig. 1b) and showed a complete tree trunk (Fig. 1c), indicating that little or no transport has occurred from their original location.

We identified the tree species of carbonized trees by analysing microscopic anatomical features of wood on three planes (cross-sectional, radial, and tangential) (see "Identifying Korean pine tree species from carbonized trees" in the Supplement for details). Of the 55 sample trees, 18 were identified as Korean pine (*Pinus koraiensis* Siebold & Zucc.) (Supplement Fig. S1). However, some small Korean pine was excluded from the chronology development, and only 19 cores from 10 Korean pines were finally used for developing chronology after the quality control of the cross-dating. Prior to performing the climate response analyses, we also sampled modern living Korean pines. Core samples from 27 living Korean pine trees located near site A (see Fig. 1a) were collected in 2013 and at a height of 1.3 m using a Pressler increment borer. We used the 19 carbonized Korean pine cores to reconstruct the climate before the Millennium Eruption (946 CE) using the current climate response of Korean pine growth.

Tree-ring width measurements and chronology development of carbonized and living samples were conducted using standard dendrochronological techniques (Cook and Kairiukstis, 2013). The carbonized and living samples were naturally air-dried. The surface of the stem cross-section of carbonized trees and the core of living trees was polished using a sandpaper-polishing machine with thick and thin brushes. Then, the tree-ring width was identified and recorded by a LINTAB 6 measuring system with an accuracy of 0.001 mm. For each carbonized tree, two cores along one line crossing the pith were measured. Quality of the cross-dating was assessed using the COFECHA programme (Holmes, 1983). Core segments having low correlation with the master chronology were excluded from the analysis. Tree-ring width

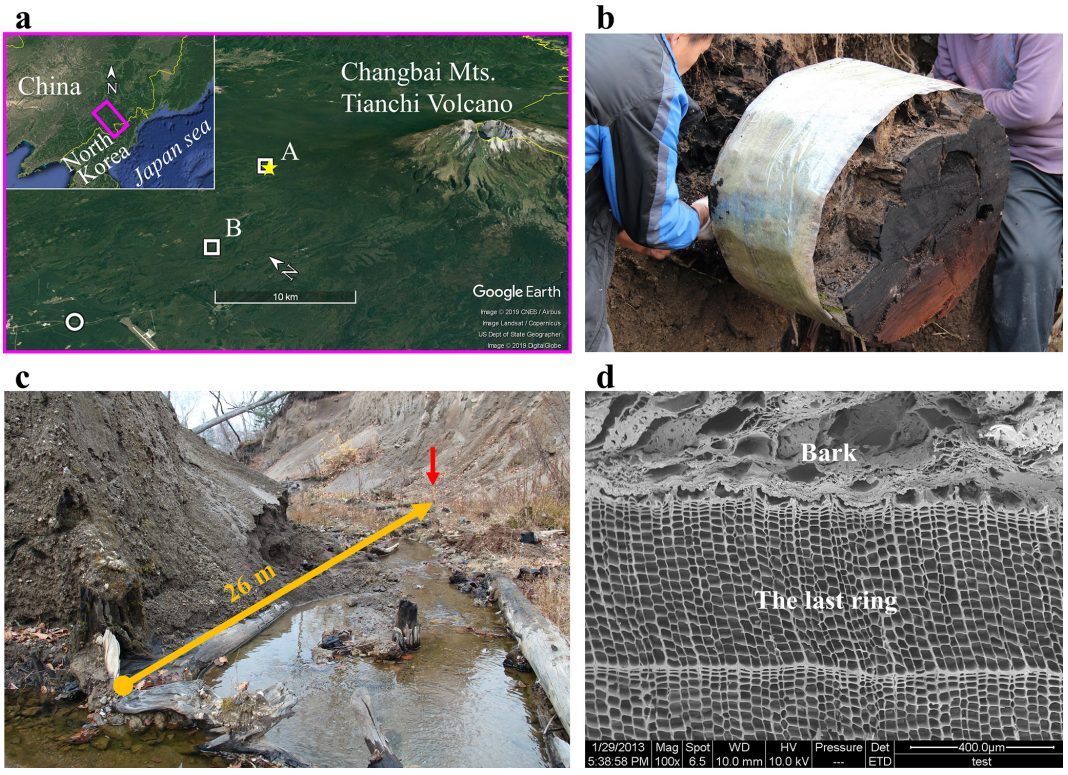

Figure 1. **(a)** Location of the Changbai Mountain and sample sites on Changbai Mountain. White squares represent sites where the carbonized logs were found (A – Weidongzhan, B – Xiaoshahe). The yellow star shows the sampling site of the modern forest. The white circle indicates the Donggang National Datum Meteorological Station. **(b, c)** Context of carbonized logs in the field. Species of logs are *Pinus koraiensis*. **(d)** Cellular characteristics of the outermost tree ring and bark of the carbonized log shown in **(b)**.

Table 1. AMS ^{14}C results of the complete outermost rings of two carbonized logs collected from Weidongzhan (site A) and Xiaoshahe (site B) on the western slope of Changbai Mountain.

Lab ID	Site	AMS ^{14}C age (yr BP)* (CE, 1σ (68.2 %))	Tree-ring calibration age (CE, 2σ (95.4 %))	Tree-ring calibration age
BA150220	A	1155 ± 20	780–790 CE (1.0 %) 820–840 CE (7.4 %) 860–900 CE (33.8 %) 910–950 CE (25.9 %)	770–970 CE (95.4 %)
BA121692	B	1090 ± 20	895–920 CE (24.8 %) 945–990 CE (43.4 %)	890–1020 CE (95.4 %)

* AMS ^{14}C ages are dated at the Peking University AMS Laboratory and given in year BP (years before 1950).

series were detrended using polynomial functions (splines with a period of 67 % of series length). However, results may be sensitive to the detrending method (Peters et al., 2015). Therefore, to ensure robustness of our results to method choice, age-detrending of the ring-width series was also performed by fitting negative exponential curves. Standardized growth chronologies were developed by calculating robust biweight means using the ARSTAN programme version 49 (Cook et al., 2017; Cook, 1985). Then, subsample signal strength (SSS) was used to evaluate the suitability and reliability of chronology data for climate reconstructions (Buras, 2017; Wigley et al., 1984). The SSS > 0.85 was used to determine the robust and maximum chronology length and to ensure the reliability of the reconstructions (Fig. S2). This threshold corresponded to a minimum sample depth of 11 samples for the carbonized tree chronology (from 745 CE) and 13 samples for the living tree chronology (from 1883 CE onwards) (Table 2). The dendrochronological characteristics of the ring-width chronologies of carbonized and living trees are shown in Table 2.

Instrumental climate data were obtained for the period 1961–2012 from the Donggang National Datum Meteorological Station (42°6′ N, 127°34.2′ E, 851 m a.s.l., situated 15–22 km apart from the sample sites; source: China Meteorological Data Network, http://data.cma.gov.cn/, last access: 26 July 2014). We calculated the Pearson correlation coefficients between the chronology and different timescale (monthly, seasonal, and annual) climate variables (precipitation, mean temperature, maximum temperature, and minimum temperature) to identify the main climate factors driving tree growth (Fig. 2). The radial growth of Korean pine was related to temperature in the pre-growing season onward (Wang et al., 2017; Zhu et al., 2009) and until the end of the growing season (September). Moreover, climate may show time-lag effects on tree radial growth (Zhou et al., 2022). Therefore, correlations were calculated from the previous April to the current September (Fig. 2). Besides, to remove the trend effects, the correlation coefficients between the first-order difference series of chronology and climate variables were also calculated to further explore their relationships (Fig. S3).

We used a linear regression model to reconstruct past climate from the tree-ring chronology. The reliability of the regression model was evaluated using split sample calibration–validation statistics whereby calibration was conducted for 1961–1986 and validation was done for 1987–2012, after which the periods were switched and the process repeated (Table 3). Model statistics included the Pearson correlation coefficient, coefficient of determination (R^2), reduction of error (RE), coefficient of efficiency (CE), Durbin–Watson text (DW), root mean square error (RMSE), and mean absolute error (MAE). Any positive RE/CE is generally accepted as indicative of reasonable skill in the reconstructions (Cook et al., 1994; Briffa et al., 1988; Fritts, 1976). The DW statistic tests the temporal autocorrelation in the residuals between modelled and observed climate data.

Correlation, R^2, and DW were calculated between instrumental April temperature and tree-ring width chronology. Reduction of error (RE), coefficient of efficiency (CE), root mean square error (RMSE), and mean absolute error (MAE) were calculated between instrumental and reconstructed April temperatures.

To analyse the abrupt changes in temperature between both periods, we calculated the changes in mean state of temperature reconstructions using a heuristic segmentation algorithm (the imposed minimum length of segments is 45 years) developed by Bernaola-Galván et al. (2001). This method has been widely used to determine the abrupt changes in mean state of a chronology (Gong et al., 2006). The significance of the changes was estimated by the t test.

Power spectrum analysis was applied to investigate the reasonable periodicities in our climate reconstructions. We used the wavelet analysis with a Morlet wavelet to examine the periodicity of the reconstructed series and to check how periodicity changes through time (Torrence and Compo, 1998). This analysis was separately performed over the two ranges of the reconstructions. We also used the cross-wavelet transform analysis (Grinsted et al., 2004) to reveal the correlation and consistency of the periodicity of mean air temperature of Changbai Mountain during 1961–2012 and mean sea surface temperature (SST) of eastern tropical Pacific (0 to 10° S and 90 to 80° W) time series (https://psl.noaa.gov/data/timeseries/monthly/NINO12/, last access: 3 April 2023). These analyses were carried out using the Matlab R2019b software.

3 Results and discussion

3.1 Temperature reconstruction

Precipitation in all months (except July) and seasons showed no significant correlation with the chronology (Fig. 2a). This was expected since the study area is wet, and moisture deficits that limit plant growth are uncommon. In contrast, some monthly, seasonal, and annual mean temperatures significantly affected the growth of Korean pine, especially for the mean temperature in April, which showed a significant ($p < 0.001$) positive correlation ($r = 0.45$) with the chronology during 1961–2012 (Fig. 2b), indicating that the radial growth of Korean pine is primarily limited by temperature in the month preceding cambial onset. Interestingly, the correlation coefficient between the chronology and April mean temperature did not change ($p > 0.01$) during 1961–2012 in Changbai Mountain (Fig. S4). The radial growth of Korean pine was also mostly significantly correlated to the maximum and minimum temperatures in April (Fig. 2cd). Similar results were found when the tree-ring width was detrended by fitting the negative exponential curves (Fig. S5). Moreover, the correlation coefficients for the first-order difference series indicated that chronologies still have a statistically significant and the strongest relationship with April temperature (Fig. S3). These are similar to the findings for Korean pine growth found in the north of Changbai Mountain (Zhu et al., 2009) and more broadly across Northeast Asia (Wang et al., 2017). Other species in other cold regions show consistent growth responses to pre-growth temperature as a limiting factor in annual radial growth (e.g. Hinoki cypress (*Chamaecyparis obtuse*) in central Japan (Yonenobu and Eckstein, 2006), Georgei fir (*Abies georgei*) in the southeastern Tibetan Plateau (Liang et al., 2009), and Scots pine (*Pinus sylvestris L.*) in northern Poland Koprowski et al., 2012). A positive growth response to April temperature can occur due to warming in the period prior to the growing season causing tree dormancy to break early, accelerating the division and enlargement of cambial cells, and extending the length of the growing season (Schweingruber, 1996). The correlation between the chronology and spring temperature is also significant, mainly due to the effects of April temperature (Fig. 2bc).

Table 2. Dendrochronological characteristics of the chronologies of carbonized and living trees.

Parameters	Carbonized trees	Modern living trees
Number of cores/trees	19/10	46/24
Time span (SSS > 0.85, year)	745–946	1883–2012
Mean sensitivity	0.163	0.226
Standard deviation	0.288	0.307
First-order autocorrelation coefficient	0.737	0.550
Correlation coefficients of all sequence	0.457	0.210
Mean correlation coefficient in a tree	0.591	0.507
Mean correlation coefficient between trees	0.390	0.194
Signal to noise ratio	3.368	3.450
Variance in first eigenvector (%)	59.7	27.9

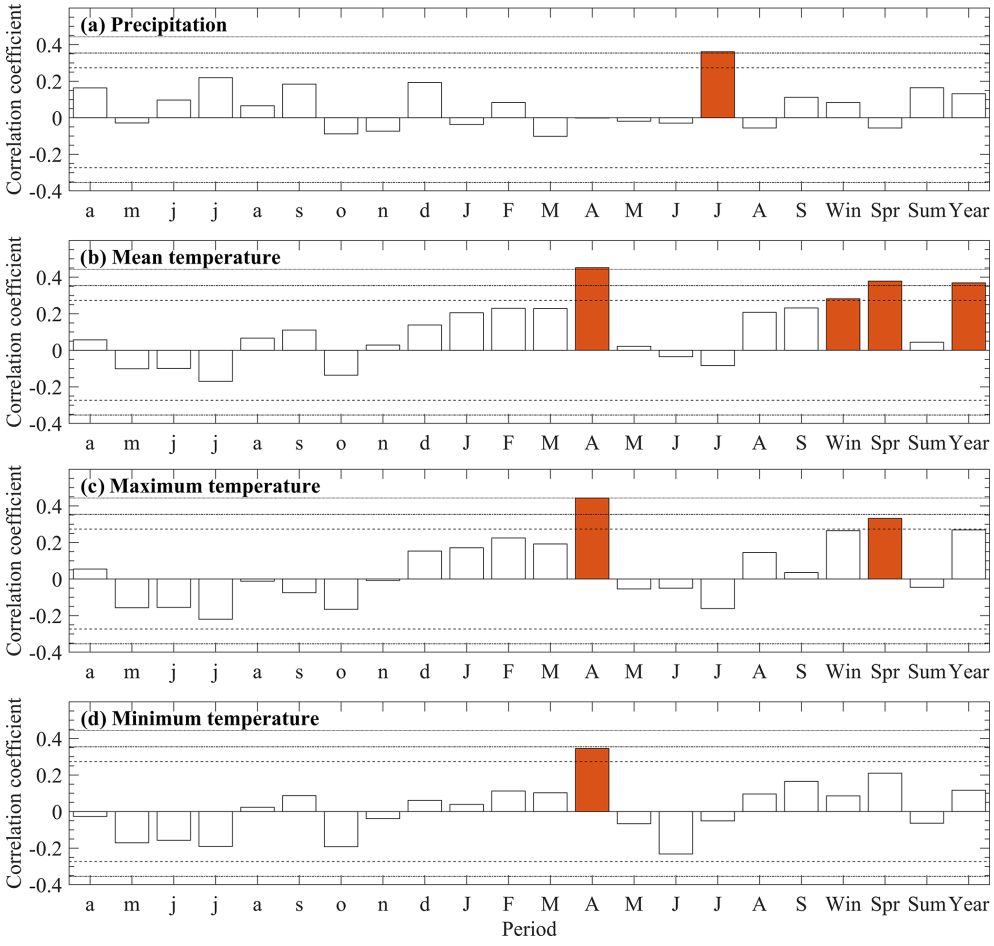

Figure 2. Pearson correlation coefficients between the tree-ring chronology and monthly, seasonal, and annual **(a)** precipitation, **(b)** mean temperature, **(c)** maximum temperature, and **(d)** minimum temperature during 1961–2012. Lowercase and uppercase letter on the x axis indicate the months of the previous and current year, respectively. The horizontal dotted, dash-dotted, and dashed lines represent significance levels of 0.001, 0.01, and 0.05, respectively. Bars with significant correlation are filled with red colour.

Table 3. Calibration/verification statistics of the temperature reconstruction.

	Calibration 1961–1986	Verification 1987–2012	Calibration 1987–2012	Verification 1961–1986	Calibration 1961–2012
Years	26	26	26	26	52
Correlation	0.42	0.45	0.45	0.42	0.45
R^2	0.18	0.20	0.20	0.18	0.20
RE	–	0.25	–	0.24	–
CE	–	0.19	–	0.17	–
DW	2.12	1.88	1.88	2.12	2.01
RMSE	1.51	1.61	1.60	1.51	1.56
MAE	1.27	1.25	1.25	1.28	1.26

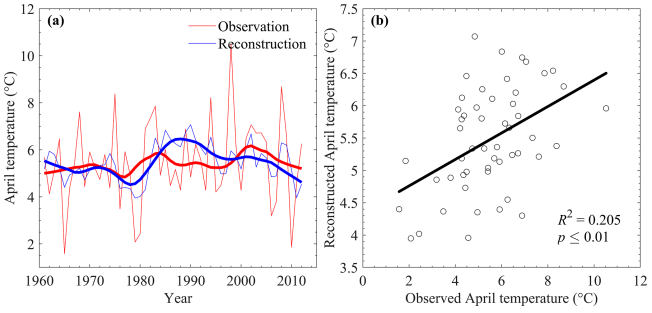

Figure 3. **(a)** Observed (thin red line) and reconstructed (thin blue line) annual April temperature. Heavy lines are the corresponding 13-year moving averaged temperatures. **(b)** Linear regression between observed and reconstructed temperatures during the period 1961–2012.

The positive RE (0.25) and CE (0.19) statistics for the late verification period and positive RE (0.24) and CE (0.17) statistics for the early verification period indicated reasonable reconstruction skill for both compared subperiods (Table 3). Therefore, we used the full calibration period for developing the April temperature model by calculating the model R^2, DW (Durbin–Watson statistic), RMSE, and MAE (Table 3). The DW statistic is calculated over the full calibration period ($DW_{1961–2012} = 2.01$, $p < 0.01$), achieving a value very close to the optimal value of 2 which indicates no significant autocorrelation in the residuals. The full tree-ring model predicting April temperature was given as

$$y = 4.34 \cdot \mathrm{CHRON} + 1.33 \quad (1)$$

where y is April temperature, and CHRON is the standardized tree-ring width index, being the model and the predictor variables significant at $p < 0.01$. The comparison between the reconstructed and instrumental April temperature is shown in Fig. 3. The reconstructed April mean temperature shows a decreasing trend after 2000, which is different from the results of reconstructed April–July minimum temperature by Lyu et al. (2016) and February–April temperature by Zhu et al. (2009). However, the decreasing trend is coincident with the change in the observed April temperature (Fig. 3a). Therefore, the difference of the change in temperature during the last decade between the temperature reconstructions may be due to seasonal diversity or regional difference. Besides, although the reconstruction underestimates the extreme temperatures recorded in some years (e.g. 1965 and 1998), it successfully captures both high- and low-frequency variations of temperature variability (Fig. 3a).

3.2 Comparisons between changes in palaeoclimate and modern climate

Based on the regression model, we reconstructed the annual April temperature and a 13-year moving average for the periods 652–946 and 1830–2012 CE (Fig. 4a). Truncated periods of reconstructions where SSS is > 0.85 were 745–946 and 1883–2012 CE. Our temperature reconstructions did not match well with the previous temperature reconstructions using the varved sediment in Lake Sihailongwan in Changbai Mountain (Chu et al., 2012), which may be due to age model error inherent in radiocarbon-dated records (Conroy et al., 2010). However, both temperature reconstructions showed coincident decreasing–increasing–decreasing variation during 850–946 CE. For regional scale, our temperature reconstructions generally coincided with the variations of pre-millennial temperature in China (Yang et al., 2002). Interestingly, variations in April temperature reconstructions during both periods in this study are similar to those observed in summer temperature reconstructions for the Northern Hemisphere (Guillet et al., 2017). These temperature reconstructions all display warm periods in 830–850, 1935–1955, and 1984–2000s CE, and they display cold periods in 1830–1840 and 1955–1983 CE.

The standard deviation (SD) of reconstructed mean April temperature was 0.61 °C during the last 100 years (847–946 CE) before the Millennium Eruption, whereas the standard deviation was 0.69 °C for the last 100 years (1913–2012 CE). That is, temperature variance (standard deviation) increased with 13 % for modern temperature in comparison to the temperature prior to the 946 CE Millennium Eruption. Moreover, the 30-year moving standard deviations showed periodical change and smaller values during the pre-eruption

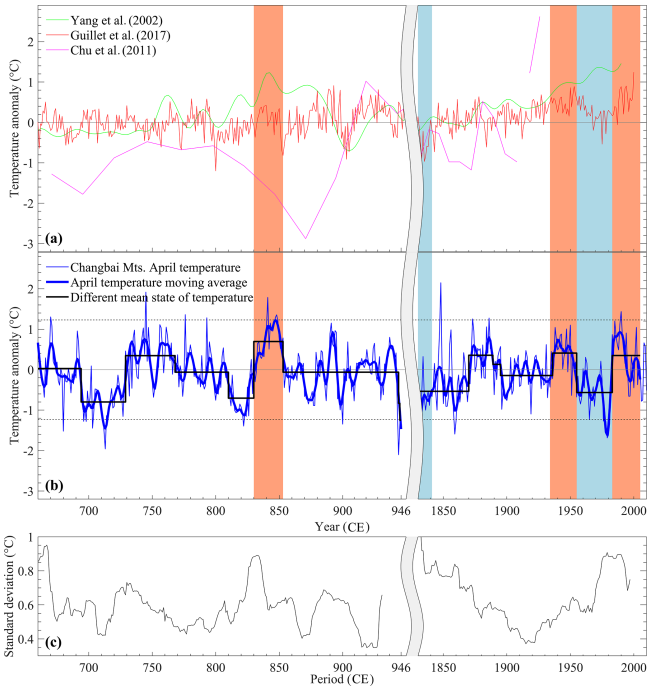

Figure 4. Anomaly of reconstructed temperature in 652–946 CE and 1830–2012 CE for different regions. **(a)** Long-term standardized temperature anomalies in China ("H-res") (green lines) (Yang et al., 2002), summer temperature anomalies for the Northern Hemisphere (red lines) (Guillet et al., 2017), and temperature anomalies using the varved sediment in Lake Sihailongwan in Changbai Mountain (magenta lines) (Chu et al., 2012). **(b)** Reconstruction of the April temperature anomaly (thin blue lines) with a 13-year moving average (bold blue lines) for Changbai Mountain in this study. The temperature anomaly is relative to the mean during the entire period. Bold black lines show the changes in mean state of the April temperature reconstructions. **(c)** Time series of standard deviation of 30-year moving window for the April temperature reconstructions in this study. A given period (e.g. 900 CE) represents a standard deviation in 30 years before and after that period (e.g. 886–915 CE).

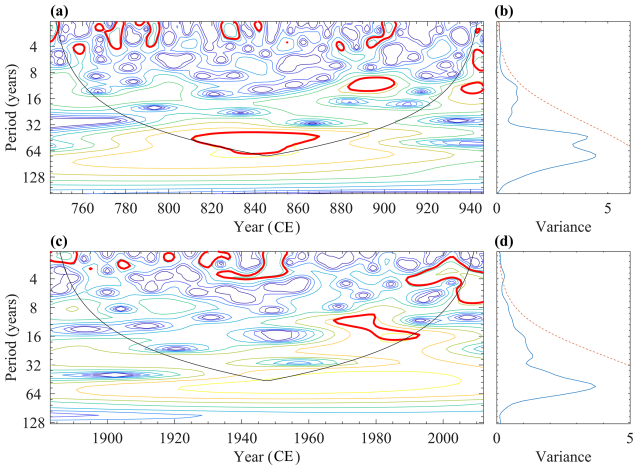

Figure 5. **(a, c)** Wavelet power spectrum of the reconstructed April temperature from **(a)** carbonized and **(c)** modern trees. The power has been scaled by the global wavelet spectrum. The bold red contour is the 95% confidence level using a red-noise (autoregressive lag1) background spectrum. **(b, d)** The global wavelet power spectrum (light blue line) for **(b)** carbonized-tree-based and **(d)** modern-tree-based temperature reconstruction. Dashed lines represent a significance of 0.05.

period than those in the last 170 years (Fig. 4b). Specifically, the 30-year moving temperature variance showed significant ($p < 0.05$) periodicity of 50–70 years (Fig. S6ab). However, there was no significant periodicity of temperature variance during the last 170 years (Fig. S6cd).

There were only 5 periods with significant differences in mean state of temperature during the last ~ 200 years before the volcano eruption (Fig. 4a). The significantly warm period in 830–850 CE was also widely recognized as the warm epoch by other temperature reconstructions for the Northern Hemisphere extratropical areas (e.g. Esper et al., 2002). In contrast, 7 periods with significantly different mean temperature states were revealed during the last ~ 170 years before present. Moreover, 5 warm years (defined as > 1.5 SD; years: 776, 793, 841, 847, 848) and 4 cold years (defined as < 1.5 SD; years: 822, 900, 944, 945) were identified during the last 200 years before the Millennium Eruption, whereas 4 warm years (1848, 1873, 1886, 1990) and 10 cold years (1859, 1860, 1965, 1976, 1977, 1978, 1979, 1980, 1981, 2011) were identified during the last 170 years before present (Fig. 4a).

These differences may be partly due to the anthropogenic influences since approximately the beginning of the Industrial Revolution (Gong et al., 2006). For example, the probability of present-day hot extremes increased with 1 %–1.2 % relative to the pre-Industrial Revolution time in the region of Changbai Mountain. Presently, 75 % of the moderate hot extremes occurring worldwide are attributable to climate warming, of which the majority are extremely likely to be anthropogenic (Fischer and Knutti, 2015). Thirty-year standard deviations during the last 170 years that are higher than the pre-eruption period may also support the attribution to increased anthropogenic influences on thermal conditions (Fig. 4b).

Wavelet analysis indicated significant ($p < 0.05$) periodicity of 3 to 4 years during 770–946 CE (Fig. 5a, b). Similar periodicities of 3 to 4 years were also found in previous analyses of instrumental and reconstructed temperatures (Zhang et al., 2013; Yu et al., 2013; Chen et al., 2010). Although our temperature reconstructions did not contain the significant ($p < 0.05$) quasi-11-year periodicity (e.g. Li et al., 2011) during the entire period, the significant ($p < 0.05$) quasi-11-year periodicity in 880–910 CE and the non-significant quasi-11-year period in 840–870 CE were found. Significantly short periodicities are typically associated with El Niño–Southern Oscillation (ENSO) (Stone et al., 1998; Allan et al., 1996), and temperature in March to May in Northeast China is affected by ENSO (Yuan and Yang, 2012). Moreover, the

changes in temperature in Northeast China correspond to the quasi-4-year changes in sea surface temperature in the central and eastern Pacific Ocean, suggesting a close link between temperature variation in Northeast China and the ENSO cycle (Zhu et al., 2004). For example, the significant ($p < 0.05$) quasi-4-year periodicity was found during the last ~ 120 years in Changbai Mountain (Fig. 5c, d). Moreover, the cross wavelet transform analysis showed that there was significant high common power in a quasi-4-year band for three periods during 1961–2012 for temperature in Changbai Mountain and sea surface temperature in eastern tropical Pacific (Fig. S7). These results indicate that the effects of some large-scale oscillations (e.g. ENSO) on palaeotemperature and modern temperature continue to be important to the climate forcing in the region of Changbai Mountain.

4 Conclusions

We presented a new 202-year reconstruction of April temperature before the Millennium Eruption occurred in 946 CE at Changbai Mountain using unique tree-ring proxies of carbonized logs buried in the tephra, which were compared to that of living trees growing during the last 130 years. Temperature reconstructions correspond well with previous large-regional temperature reconstructions. Our results showed that, although the influences of some internal variability (e.g. ENSO) on variation in temperature do not change between the periods, the changes in modern temperatures become more complex (e.g. increased variation, abrupt changes, and weakening in periodicity of temperature variance) than those in period prior to 946 CE, likely due to anthropogenic influences. The present study provides tree-ring proxies for climate reconstructions in Northeast Asia for the last millennium. Documentation of these features is important for understanding long-term regional climate dynamics and analysing the millennial-scale changes in vegetation–climate relationship in Northeast Asia.

Data availability. Tree-ring chronology and climate data used in this study are archived at ZENODO: https://doi.org/10.5281/zenodo.6633856 (Du and Wu, 2020). They can also be provided by the corresponding author.

Supplement. The supplement related to this article is available online at: https://doi.org/10.5194/cp-19-1295-2023-supplement.

Author contributions. HD, ZW, and HSH conceived and led this study. Tree rings and observation data collection was led by HD and SZ. Analyses and the first draft was carried out by HD and MS, and all authors contributed to revising subsequent drafts.

Competing interests. The contact author has declared that none of the authors has any competing interests.

Disclaimer. Publisher's note: Copernicus Publications remains neutral with regard to jurisdictional claims in published maps and institutional affiliations.

Financial support. This research has been supported by the National Natural Science Foundation of China (grant nos. 42271100 and U19A2023) and the Fundamental Research Funds for the Central Universities (grant no. 2412020FZ002).

Review statement. This paper was edited by Mary Gagen and reviewed by two anonymous referees.

References

Allan, R., Lindesay, J., and Parker, D.: El Niño southern oscillation & climatic variability, CSIRO Publishing, Collingwood, 405 pp., ISBN 9780643058033, 1996.

Bernaola-Galván, P., Ivanov, P. C., Nunes Amaral, L. A., and Stanley, H. E.: Scale Invariance in the Nonstationarity of Human Heart Rate, Phys. Rev. Lett., 87, 168105, https://doi.org/10.1103/PhysRevLett.87.168105, 2001.

Briffa, K. R., Jones, P. D., Pilcher, J. R., and Hughes, M. K.: Reconstructing Summer Temperatures in Northern Fennoscandinavia Back to A.D. 1700 Using Tree-Ring Data From Scots Pine, Arct. Alp. Res., 20, 385–394, https://doi.org/10.1080/00040851.1988.12002691, 1988.

Büntgen, U., Wacker, L., Nicolussi, K., Sigl, M., Güttler, D., Tegel, W., Krusic, P. J., and Esper, J.: Extraterrestrial confirmation of tree-ring dating, Nat. Clim. Change, 4, 404, https://doi.org/10.1038/nclimate2240, 2014.

Buras, A.: A comment on the expressed population signal, Dendrochronologia, 44, 130–132, https://doi.org/10.1016/j.dendro.2017.03.005, 2017.

Chen, S., Shi, Y., Guo, Y., and Zheng, Y.: Temporal and spatial variation of annual mean air temperature in arid and semiarid region in northwest China over a recent 46 year period, J. Arid Land, 2, 87–97, 2010.

Chen, X.-Y., Blockley, S. P. E., Tarasov, P. E., Xu, Y.-G., McLean, D., Tomlinson, E. L., Albert, P. G., Liu, J.-Q., Müller, S., Wagner, M., and Menzies, M. A.: Clarifying the distal to proximal tephrochronology of the Millennium (B–Tm) eruption, Changbaishan Volcano, northeast China, Quat. Geochronol., 33, 61–75, https://doi.org/10.1016/j.quageo.2016.02.003, 2016.

Chu, G., Sun, Q., Wang, X., Liu, M., Lin, Y., Xie, M., Shang, W., and Liu, J.: Seasonal temperature variability during the past 1600 years recorded in historical documents and varved lake sediment profiles from northeastern China, Holocene, 22, 785–792, https://doi.org/10.1177/0959683611430413, 2012.

Conroy, J. L., Overpeck, J. T., and Cole, J. E.: El Niño/Southern Oscillation and changes in the zonal gradient of tropical Pacific sea surface temperature over the last 1.2 ka, PAGES News, 18, 32–34, 2010.

Cook, E. R.: A time series analysis approach to tree-ring standardization, Graduate College, University of Arizona, Tucson, http://hdl.handle.net/10150/188110 (last access: 3 April 2023), 1985.

Cook, E. R. and Kairiukstis, L. A.: Methods of Dendrochronology: Applications in the Environmental Sciences, Springer Netherlands, 394 pp., https://doi.org/10.1007/978-94-015-7879-0, 2013.

Cook, E. R., Briffa, K. R., and Jones, P. D.: Spatial regression methods in dendroclimatology: A review and comparison of two techniques, Int. J. Climatol., 14, 379–402, https://doi.org/10.1002/joc.3370140404, 1994.

Cook, E. R., Krusic, P. J., Peters, K., and Holmes, R. L.: Program ARSTAN (version 49), Autoregressive tree–ring standardization program, Tree–Ring Laboratory of Lamont–Doherty Earth Observatory, USA, https://www.geog.cam.ac.uk/research/projects/dendrosoftware/ (last access: 21 November 2022), 2017.

Cui, Z., Zhang, S., and Tian, J.: The study on volcanic eruption and forest conflagration since holocene quaternary in Changbai Mt., Geogr. Res., 16, 92–97, 1997.

Ding, Y., Ren, G., Zhao, Z., Xu, Y., Luo, Y., Li, Q., and Zhang, J.: Detection, causes and projection of climate change over China: An overview of recent progress, Adv. Atmos. Sci., 24, 954–971, https://doi.org/10.1007/s00376-007-0954-4, 2007.

Du, H. and Wu, Z.: Data for publication "A comparison of pre-Millennium eruption (946 AD) and modern temperatures from tree rings in the Changbai Mountain, northeast Asia", Zenodo [data set], https://doi.org/10.5281/zenodo.6633856, 2020.

Du, H., Liu, J., Li, M.-H., Büntgen, U., Yang, Y., Wang, L., Wu, Z., and He, H. S.: Warming-induced upward migration of the alpine treeline in the Changbai Mountains, northeast China, Glob. Change Biol., 24, 1256–1266, https://doi.org/10.1111/gcb.13963, 2018.

Du, H., Li, M.-H., Rixen, C., Zong, S., Stambaugh, M., Huang, L., He, H. S., and Wu, Z.: Sensitivity of recruitment and growth of alpine treeline birch to elevated temperature, Agr. Forest Meteorol., 304–305, 108403, https://doi.org/10.1016/j.agrformet.2021.108403, 2021.

Esper, J., Cook, E. R., and Schweingruber, F. H.: Low-Frequency Signals in Long Tree-Ring Chronologies for Reconstructing Past Temperature Variability, Science, 295, 2250–2253, https://doi.org/10.1126/science.1066208, 2002.

Fischer, E. M. and Knutti, R.: Anthropogenic contribution to global occurrence of heavy-precipitation and high-temperature extremes, Nat. Clim. Change, 5, 560, https://doi.org/10.1038/nclimate2617, 2015.

Fritts, H. C.: Tree rings and climate, Elsevier, New York, ISBN 978-0-12-268450-0, https://doi.org/10.1016/B978-0-12-268450-0.X5001-0, 1976.

Gong, Z.-Q., Feng, G.-L., Wan, S.-Q., and Li, J.-P.: Analysis of features of climate change of Huabei area and the global climate change based on heuristic segmentation algorithm, Acta Phys. Sinica, 55, 477, https://doi.org/10.7498/aps.55.477, 2006.

Grinsted, A., Moore, J. C., and Jevrejeva, S.: Application of the cross wavelet transform and wavelet coherence to geophysical time series, Nonlin. Processes Geophys., 11, 561–566, https://doi.org/10.5194/npg-11-561-2004, 2004.

Guillet, S., Corona, C., Stoffel, M., Khodri, M., Lavigne, F., Ortega, P., Eckert, N., Sielenou, P. D., Daux, V., Churakova , Olga V., Davi, N., Edouard, J.-L., Zhang, Y., Luckman, Brian H., Myglan, V. S., Guiot, J., Beniston, M., Masson-Delmotte, V., and Oppenheimer, C.: Climate response to the Samalas volcanic eruption in 1257 revealed by proxy records, Nat. Geosci., 10, 123, https://doi.org/10.1038/ngeo2875, 2017.

Holmes, R. L.: Computer-assisted quality control in tree-ring dating and measurement, Tree-Ring Bull., 43, 69–78, 1983.

Horn, S. and Schmincke, H.-U.: Volatile emission during the eruption of Baitoushan Volcano (China/North Korea) ca. 969 AD, B. Volcanol., 61, 537–555, https://doi.org/10.1007/s004450050004, 2000.

IPCC: Summary for Policymakers. In: Climate Change 2021: The Physical Science Basis. Contribution of Working Group I to the Sixth Assessment Report of the Intergovernmental Panel on Climate Change, edited by: Masson-Delmotte, V., Zhai, P., Pirani, A., Connors, S. L., Péan, C., Berger, S., Caud, N., Chen, Y., Goldfarb, L., Gomis, M. I., Huang, M., Leitzell, K., Lonnoy, E., Matthews, J. B. R., Maycock, T. K., Waterfield, T., Yelekçi, O., Yu, R., and Zhou, B., Cambridge University Press, Cambridge, United Kingdom and New York, NY, USA, 3–32, https://www.ipcc.ch/report/ar6/wg1/ (last access: 10 September 2021), 2021.

Koprowski, M., Przybylak, R., Zielski, A., and Pospieszyńska, A.: Tree rings of Scots pine (Pinus sylvestris L.) as a source of information about past climate in northern Poland, Int. J. Biometeorol., 56, 1–10, https://doi.org/10.1007/s00484-010-0390-5, 2012.

Li, Z., Shi, C. M., Liu, Y., Zhang, J., Zhang, Q., and Ma, K.: Summer mean temperature variation from 1710–2005 inferred from tree-ring data of the Baimang Snow Mountains, northwestern Yunnan, China, Clim. Res., 47, 207–218, https://doi.org/10.3354/cr01012, 2011.

Liang, E. Y., Shao, X. M., and Xu, Y.: Tree-ring evidence of recent abnormal warming on the southeast Tibetan Plateau, Theor. Appl. Climatol., 98, 9–18, https://doi.org/10.1007/s00704-008-0085-6, 2009.

Ljungqvist, F. C.: A new reconstruction of temperature variability in the extra-tropical northern hemisphere during the last two millennia, Geogr. Ann. A , 92, 339–351, https://doi.org/10.1111/j.1468-0459.2010.00399.x, 2010.

Lyu, S., Li, Z., Zhang, Y., and Wang, X.: A 414-year tree-ring-based April–July minimum temperature reconstruction and its implications for the extreme climate events, northeast China, Clim. Past, 12, 1879–1888, https://doi.org/10.5194/cp-12-1879-2016, 2016.

Mann, M. E. and Jones, P. D.: Global surface temperatures over the past two millennia, Geophys. Res. Lett., 30, 1820, https://doi.org/10.1029/2003GL017814, 2003.

Mann, M. E., Bradley, R. S., and Hughes, M. K.: Northern hemisphere temperatures during the past millennium: inferences, uncertainties, and limitations, Geophys. Res. Lett., 26, 759–762, 1999.

Mann, M. E., Zhang, Z., Hughes, M. K., Bradley, R. S., Miller, S. K., Rutherford, S., and Ni, F.: Proxy-based reconstructions of hemispheric and global surface temperature variations over the past two millennia, P. Natl. Acad. Sci. USA, 105, 13252, https://doi.org/10.1073/pnas.0805721105, 2008.

Moberg, A., Sonechkin, D. M., Holmgren, K., Datsenko, N. M., and Karlén, W.: Highly variable Northern Hemisphere temperatures reconstructed from low- and high-resolution proxy data, Nature, 433, 613–617, https://doi.org/10.1038/nature03265, 2005.

Oppenheimer, C., Wacker, L., Xu, J., Galván, J. D., Stoffel, M., Guillet, S., Corona, C., Sigl, M., Di Cosmo, N., Hajdas, I., Pan, B., Breuker, R., Schneider, L., Esper, J., Fei, J., Hammond, J. O. S., and Büntgen, U.: Multi-proxy dating the 'Millennium Eruption' of Changbaishan to late 946 CE, Quaternary Sci. Rev., 158, 164–171, https://doi.org/10.1016/j.quascirev.2016.12.024, 2017.

PAGES 2k Consortium: Continental-scale temperature variability during the past two millennia, Nat. Geosci., 6, 339, https://doi.org/10.1038/ngeo1797, 2013.

Peters, R. L., Groenendijk, P., Vlam, M., and Zuidema, P. A.: Detecting long-term growth trends using tree rings: a critical evaluation of methods, Glob. Change Biol., 21, 2040–2054, https://doi.org/10.1111/gcb.12826, 2015.

Schneider, L., Smerdon, J. E., Büntgen, U., Wilson, R. J. S., Myglan, V. S., Kirdyanov, A. V., and Esper, J.: Revising midlatitude summer temperatures back to A.D. 600 based on a wood density network, Geophys. Res. Lett., 42, 4556–4562, https://doi.org/10.1002/2015GL063956, 2015.

Schweingruber, F. H.: Tree rings and environment: dendroecology, Paul Haupt AG Bern, Berne, 609 pp., ISBN 3 258 05458 4, https://doi.org/10.1111/j.1469-8137.1998.149-8.x, 1996.

Shao, X. M. and Wu, X. D.: Reconstruction of climate change on Changbai Mountain, northeast China using tree-ring data, Quaternary Science, 1, 76–85, 1997 (in Chinese with English abstract).

Stone, L., Saparin, P. I., Huppert, A., and Price, C.: El Niño Chaos: The role of noise and stochastic resonance on the ENSO cycle, Geophys. Res. Lett., 25, 175–178, https://doi.org/10.1029/97GL53639, 1998.

Sun, C., You, H., Liu, J., Li, X., Gao, J., and Chen, S.: Distribution, geochemistry and age of the Millennium eruptives of Changbaishan volcano, Northeast China – A review, Front. Earth Sci., 8, 216–230, https://doi.org/10.1007/s11707-014-0419-x, 2014.

Torrence, C. and Compo, G. P.: A Practical Guide to Wavelet Analysis, B. Am. Meteorol. Soc., 79, 61–78, https://doi.org/10.1175/1520-0477(1998)079<0061:APGTWA>2.0.CO;2, 1998.

Wang, J., Yang, B., Osborn, T. J., Ljungqvist, F. C., Zhang, H., and Luterbacher, J.: Causes of East Asian Temperature Multidecadal Variability Since 850 CE, Geophys. Res. Lett., 45, 13485–13494, https://doi.org/10.1029/2018GL080725, 2018.

Wang, X., Zhang, M., Ji, Y., Li, Z., Li, M., and Zhang, Y.: Temperature signals in tree-ring width and divergent growth of Korean pine response to recent climate warming in northeast Asia, Trees, 31, 415–427, https://doi.org/10.1007/s00468-015-1341-x, 2017.

Wei, H., Sparks, R. S. J., Liu, R., Fan, Q., Wang, Y., Hong, H., Zhang, H., Chen, H., Jiang, C., Dong, J., Zheng, Y., and Pan, Y.: Three active volcanoes in China and their hazards, J. Asian Earth Sci., 21, 515–526, https://doi.org/10.1016/S1367-9120(02)00081-0, 2003.

Wigley, T. M. L., Briffa, K. R., and Jones, P. D.: On the Average Value of Correlated Time Series, with Applications in Dendroclimatology and Hydrometeorology, J. Clim. Appl. Meteorol., 23, 201–213, https://doi.org/10.1175/1520-0450(1984)023<0201:OTAVOC>2.0.CO;2, 1984.

Xu, J., Pan, B., Liu, T., Hajdas, I., Zhao, B., Yu, H., Liu, R., and Zhao, P.: Climatic impact of the Millennium eruption of Changbaishan volcano in China: New insights from high-precision radiocarbon wiggle-match dating, Geophys. Res. Lett., 40, 54–59, https://doi.org/10.1029/2012GL054246, 2013.

Yang, B., Braeuning, A., Johnson, K. R., and Shi, Y.: General characteristics of temperature variation in China during the last two millennia, Geophys. Res. Lett., 29, L014485, https://doi.org/10.1029/2001GL014485, 2002.

Yin, J., Jull, A. J. T., Burr, G. S., and Zheng, Y.: A wiggle-match age for the Millennium eruption of Tianchi Volcano at Changbaishan, Northeastern China, Quaternary Sci. Rev., 47, 150–159, https://doi.org/10.1016/j.quascirev.2012.05.015, 2012.

Yonenobu, H. and Eckstein, D.: Reconstruction of early spring temperature for central Japan from the tree-ring widths of Hinoki cypress and its verification by other proxy records, Geophys. Res. Lett., 33, L10701, https://doi.org/10.1029/2006GL026170, 2006.

Yu, S., Yuan, Y., Wei, W., Chen, F., Zhang, T., Shang, H., Zhang, R., and Qing, L.: A 352-year record of summer temperature reconstruction in the western Tianshan Mountains, China, as deduced from tree-ring density, Quaternary Res., 80, 158–166, https://doi.org/10.1016/j.yqres.2013.05.005, 2013.

Yuan, Y. and Yang, S.: Impacts of Different Types of El Niño on the East Asian Climate: Focus on ENSO Cycles, J. Climate, 25, 7702–7722, https://doi.org/10.1175/JCLI-D-11-00576.1, 2012.

Yun, S.-H.: Volcanological Interpretation of Historical Eruptions of Mt. Baekdusan Volcano, J. Korean Earth Sci. Soc., 34, 456–469, 2013.

Zhang, T., Yuan, Y., Liu, Y., Wei, W., Zhang, R., Chen, F., Yu, S., Shang, H., and Qin, L.: A tree-ring based temperature reconstruction for the Kaiduhe River watershed, northwestern China, since A.D. 1680: Linkages to the North Atlantic Oscillation, Quat. Int., 311, 71–80, https://doi.org/10.1016/j.quaint.2013.07.026, 2013.

Zhou, Y., Liu, L., Zhang, M., and Yu, J.: Medicinal plant resources and their diversity in Changbai Mountain National Nature Reserve, Scientia Silvae Sinicae, 41, 57–64, 2005.

Zhou, Y., Yi, Y., Liu, H., Song, J., Jia, W., and Zhang, S.: Altitudinal trends in climate change result in radial growth variation of Pinus yunnanensis at an arid-hot valley of southwest China, Dendrochronologia, 71, 125914, https://doi.org/10.1016/j.dendro.2021.125914, 2022.

Zhu, H. F., Fang, X. Q., Shao, X. M., and Yin, Z. Y.: Tree ring-based February–April temperature reconstruction for Changbai Mountain in Northeast China and its implication for East Asian winter monsoon, Clim. Past, 5, 661–666, https://doi.org/10.5194/cp-5-661-2009, 2009.

Zhu, Y., Chen, L., and Yu, R.: Analysis of the relationship between the China anomalous climate variation and ENSO cycle on the quasi-four-year scale, J. Trop. Meteorol., 19, 345–356, https://doi.org/10.3969/j.issn.1006-8775.2004.01.001, 2004.